Macromolecules

pubs.acs.org/Macromolecules Article

Thermoresponsive Polymer Sorbents for Efficient Removal of Perfluorinated Compounds via Simple Heating

Xiao Tan, Yiqing Wang, Zhuojing Yang, Yutong Zhu, Chunrong Yu, Kehan Liu, Yutong He, Andrew K. Whittaker,* and Cheng Zhang*

Cite This: *Macromolecules* 2024, 57, 11166−11176 Read Online

ACCESS | Metrics & More | Article Recommendations | Supporting Information

ABSTRACT: The efficient removal of per- and polyfluoroalkyl substances (PFAS) and recycling sorbents from contaminated water face grand challenges in the field of PFAS remediation. In this work, a series of thermoresponsive perfluoropolyether (PFPE)-containing polymer sorbents were developed for efficient removal of PFAS from contaminated water using a simple heating process. The polymer sorbents are thermoresponsive due to inclusion of the monomer *N*-isopropylacrylamide (NIPAM). Four block copolymers with the same degree of polymerization (DP) of [2-(acryloyloxy)ethyl]-trimethylammonium iodide (AETAI) but increasing DPs of NIPAM were prepared via reversible addition−fragmentation chain-transfer (RAFT) polymerization. The results demonstrate that the balance between hydrophobic/hydrophilic segments from the polymers significantly influences their lower critical transition temperatures (LCSTs), and such balance could be altered by the presence of amphiphilic PFAS. Upon complete sorption, >99% removal for majority of the tested PFAS was achieved by heating the solution mixture to above its lower critical solution temperature and filtration. The study introduces the design and preparation of efficient "smart" PFAS sorbents based on their thermoresponsive properties, offering a new approach to effectively separate PFAS sorbents from treated solutions.

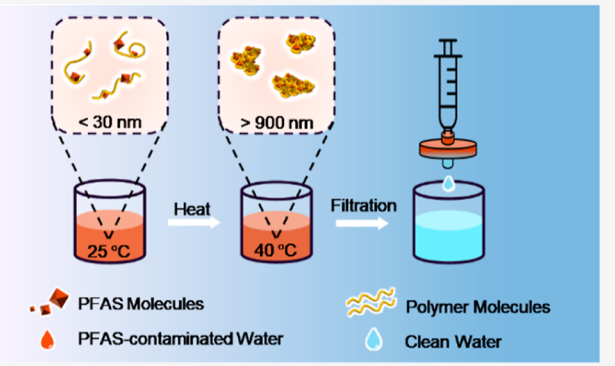

1. INTRODUCTION

Per- and polyfluoroalkyl substances (PFAS) are a group of synthetic compounds that have raised broad concerns due to their adverse effects on the environment and human health.[1,2] The presence of unique carbon−fluorine bonds makes the PFAS ultrastable, rendering them highly resistant to both environmental and metabolic degradation.[3] The bioaccumulation of PFAS in organisms and their toxicity to human body have been demonstrated,[4−10] leading to health problems such as altered thyroid hormone levels, disruption of the immune system, liver and kidney diseases, and damage to reproductive cells.

Fluorinated polymer sorbents have shown great promise for capture and removal of PFAS.[11−18] The key to their success is the participation of fluorous interactions between the fluorinated moiety of the sorbent and the perfluoroalkyl segment of PFAS, not only providing effective capture but also enhancing sorption selectivity owing to their fluorophilicity.[11,12] For example, Koda et al. developed fluorinated microgel star polymers with a condensed fluorous core via ruthenium-catalyzed living radical polymerization for removal of perfluorooctanoic acid (PFOA) from aqueous solutions.[12] The fluorous core, consisting of perfluoroalkyl methacrylate, was capable of selective capture of PFOA at an initial concentration of ∼10 mg/L (ppm), with 97.5% of PFOA being removed after sorption for 12 h.[12] Quan et al. extended the concept and prepared cross-linked fluorous-core nanoparticle-embedded hydrogels by tandem photocontrolled radical polymerization, for easier separation of the sorbent from the solution after removal of PFAS.[14] In their work, a fluorinated methacrylamide was used instead of perfluoroalkyl methacrylate to increase the stability of the PFAS sorbent. After treatment for 6 h, >99% removal of PFOA was observed for all of the three aqueous solutions with initial concentrations of 1, 100, and 1000 μg/L (ppb), while the fluorine-free hydrogel showed ∼0% removal under identical conditions,[14] highlighting the importance of fluorous interactions for effective removal of PFAS. More recently, Kumarasamy et al. prepared a cross-linked ionic fluorogel by inclusion of both cationic quaternized ammonium functional groups and perfluoropolyether (PFPE).[15] The ionic fluorogel showed

Received: August 6, 2024
Revised: October 22, 2024
Accepted: November 15, 2024
Published: November 21, 2024

Scheme 1. Synthetic Scheme for Thermoresponsive Cationic PFPE-Containing Polymer Sorbents[a]

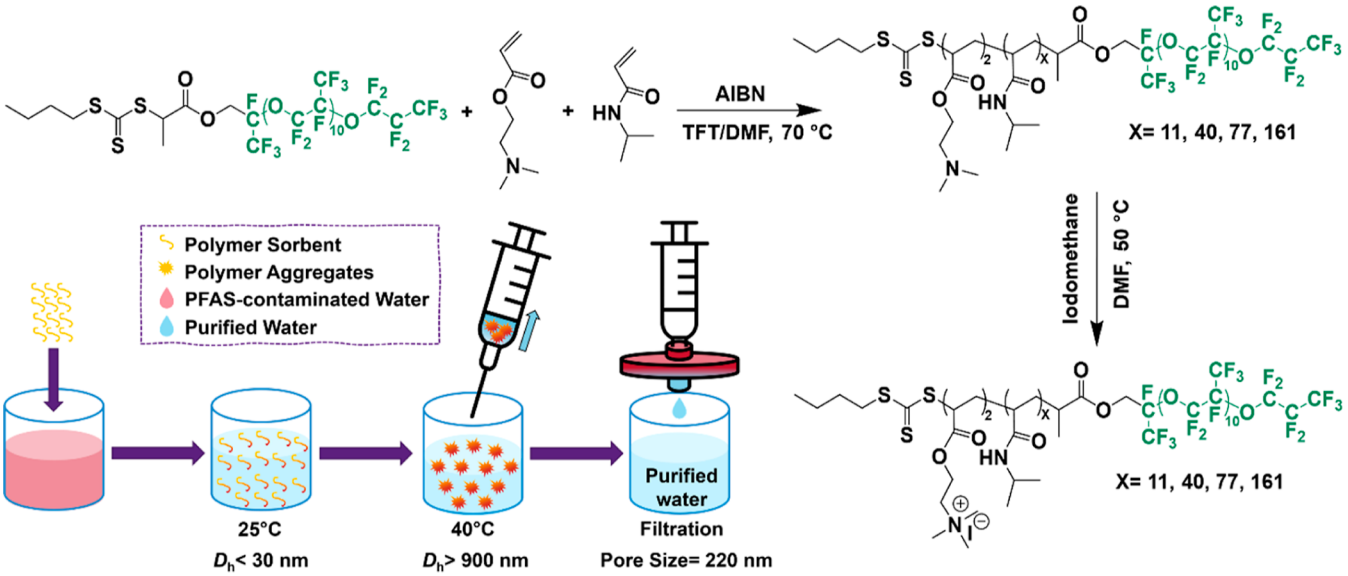

[a]Inset, schematic illustration of using thermoresponsive cationic PFPE-containing polymer sorbents for PFAS-contaminated water treatment.

94% removal of the ammonium salt of hexafluoropropylene oxide dimer acid (GenX) at an environmentally relevant concentration (1 ppb) within 30 s in water, and >80% removal of 18 different legacy and emerging PFAS at the same initial concentration, i.e., 1 ppb each from a aqueous solution collected at a water treatment plant after treatment for 2 h.[15] The above studies separated PFAS sorbents from aqueous solutions via dialysis,[12] filtration,[13,14] or centrifugation after removal of PFAS.[15] The dialysis method was applied specifically when sorbents were small particles,[12] potentially increasing the cost and making the separation process time-consuming. By designing and preparing cross-linked hydrogels with larger sizes,[13−15] either filtration or centrifugation was used, largely increasing the convenience of recycling of PFAS sorbents and their feasibility for practical use.

Thermoresponsive polymers are a class of materials that undergo reversible changes in their physical properties in response to variations in the temperature. Poly(*N*-isopropylacrylamide) (PNIPAM) is a well-studied thermoresponsive polymer that demonstrates unique behavior: it dissolves in water when the temperature is below its lower critical solution temperature (LCST) of ∼32 °C but becomes insoluble and undergoes phase transition when the temperature exceeds its LCST.[19−22] The LCST of PNIPAM polymer can be finely tuned and manipulated by incorporating other cofunctional monomers, thus alternating the hydrophilic−lipophilic balance of the copolymer.[23,24] For example, copolymerizing NIPAM with more hydrophilic monomers like 2-hydroxyethyl acrylate (HEA) raises the LCST, and an increased content of the hydrophilic comonomer further elevates the critical temperature.[25−27] Conversely, incorporating hydrophobic segments,[28,29] like fluorinated compounds, lowers the LCST. Therefore, the preparation of thermoresponsive PNIPAM PFAS capture agents presents a promising alternative strategy for separation of PFAS sorbents from the aqueous solution after removal of PFAS. Leveraging their aggregation properties under elevated temperatures could enable efficient filtration or centrifugation processes, thus enhancing the effectiveness of PFAS sorbent separation efforts.

In this work, a series of thermoresponsive block copolymers with PFPE as one block, and a statistic copolymer of [2-(acryloyloxy)ethyl]trimethylammonium iodide (AETAI) and NIPAM as the other block have been prepared via reversible addition−fragmentation chain-transfer (RAFT) polymerization. PAN161+, the polymer sorbent with the highest NIPAM (86.8 wt %) but lowest AETAI contents (2.7 wt %), showed the strongest phase transition and the lowest LCST (58 °C) in water. Our results demonstrate that PAN161+ had strong interactions with PFOA, with decreasing LCSTs of PAN161+ being observed in the presence of increasing concentrations of PFOA. Efficient removal (>99%) of the majority of 11 different PFAS at 100 ppb was achieved by heating to 40 °C and filtration. In addition, the sorbed PFAS could be released by simply heating the solution to high temperatures at >40 °C. The results provide important design criteria for thermoresponsive PFAS sorbents and prove the concept of using such type of sorbent for PFAS removal from contaminated environments.

2. RESULTS AND DISCUSSION

2.1. Design, Synthesis, and Characterization of Cationic PFPE-Containing Thermoresponsive Block Copolymer Sorbents. Results previously reported by our group have demonstrated that the inclusion of both perfluoropolyether (PFPE) and cationic functional groups are important for efficient removal of PFAS from aqueous solutions.[30,31] However, practical application of these polymer sorbents has been hindered by challenges in separating the polymer from the aqueous solution once sorption occurs. In this work, we address this issue by incorporating a thermoresponsive *N*-isopropylacrylamide (NIPAM) segment into our cationic PFPE polymers. Such modification allows easy separation of the polymer sorbent after PFAS capture by simply heating the solution mixture to a temperature above the LCST, followed by subsequent filtration. The overall synthetic scheme for the thermoresponsive cationic PFPE-containing thermoresponsive polymers is shown in Scheme 1.

https://doi.org/10.1021/acs.macromol.4c01868
Macromolecules 2024, 57, 11166−11176

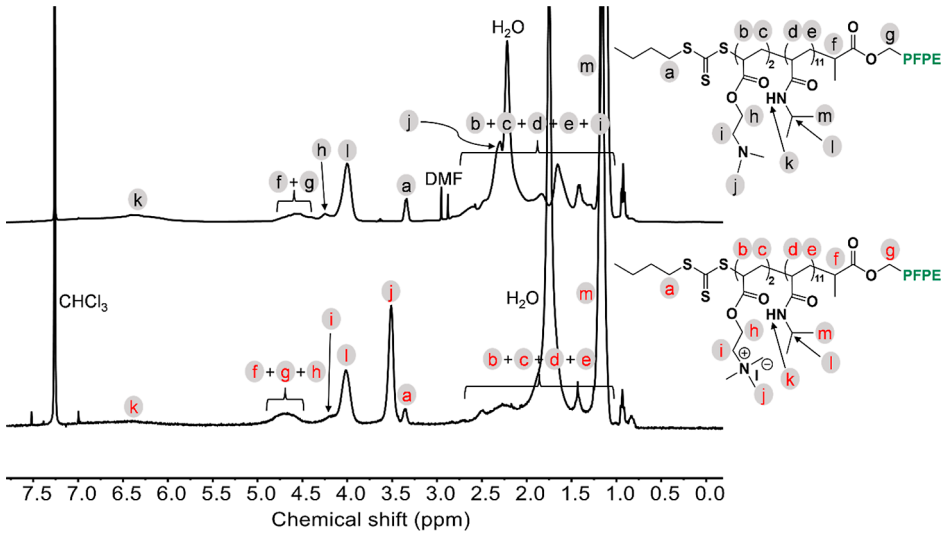

Figure 1. ^{1}H NMR spectra in $CDCl_3$ and the corresponding assignments for PAN11 (top) and PAN11+ (bottom).

The PFPE-containing macro-RAFT transfer agent was synthesized by *N*-(3-(dimethylamino)propyl)-*N*′-ethylcarbodiimide hydrochloride/4-(dimethylamino)pyridine (EDCl/DMAP) coupling esterification reaction between 2-(butylthiocarbonothioylthio)propionic acid (BTPA) and commercially available hydroxy-terminated PFPE. Both ^{1}H and ^{19}F NMR spectra confirm the successful synthesis of the PFPE-containing macro-RAFT transfer agent (Figures S1 and S2).[30,31] A series of PFPE block copolymers with the same degree of polymerization (DP) of 2-(dimethylamino)ethyl acrylate (DMAEA) (i.e., two) but increasing DP of NIPAM (i.e., 11, 40, 77, and 161) were subsequently prepared in the presence of PFPE macro-RAFT agent, namely, poly($DMAEA_2$-co-$NIPAM_{11}$)-PFPE (PAN11), poly($DMAEA_2$-co-$NIPAM_{40}$)-PFPE (PAN40), poly($DMAEA_2$-co-$NIPAM_{77}$)-PFPE (PAN77), and poly($DMAEA_2$-co-$NIPAM_{161}$)-PFPE (PAN161) (Figure S3). Again, both ^{1}H and ^{19}F NMR spectroscopy analyses indicate the successful syntheses of the four polymers after purification as all peaks in the spectra could be successfully identified and assigned (Figure 1, top; Figures S4−S6, top, and Figure S7). Taking PAN11 as an example, the single proton (1H, >CH−) from the methine group of NIPAM contributes to a single broad peak at 4.00 ppm (peak l in Figure 1, top), while another single broad peak due to the methylene protons (2H, $-CH_2O-$) next to the ester group of DMAEA was observed at 4.25 ppm (peak h, Figure 1, top).

Quaternization of the four block copolymers to produce PAN11+, PAN40+, PAN77+, and PAN161+ was achieved by addition of excess iodomethane (Figure 1, bottom; Figures S4−S6, bottom; and Figure S8). Typically, for PAN11+, the peak j due to the protons from the two methyl terminal groups of DMAEA shifted from 2.3 ppm (Figure 1, top) to 3.5 ppm after the reaction (Figure 1, bottom),[31] indicating the successful quaternization. For the other three polymers, i.e., PAN40+, PAN77+, and PAN161+ due to the much higher DP of NIPAM cf. that of DMAEA, peak j is not resolved due to overlapping with the polymer backbone peaks (peaks b to e, Figures S4−S6, top). The conversion of DMAEA to quaternary ammonium groups was determined by calculating DP of [2-(acryloyloxy)ethyl]trimethylammonium iodide (AETAI) using the methylene protons next to the sulfur from BTPA (peak a, 2H, $-CH_2S-$) and the protons from the three methyl terminal groups of AETAI side chain (peak j, 9H, $3 \times -CH_3$) in each ^{1}H spectrum (Figure 1 bottom; Figures S4−S6, bottom). The calculated DP of AETAI for each polymer generally matched the target DP of DMAEA, i.e., two, thus the conversion was considered to be ∼100% for all four polymers. Results from size exclusion chromatography (SEC) demonstrate that all four polymers had low molar mass dispersity ($Đ$< 1.2). Refer to Table 1 for a summary of the structural characterization of the four block copolymers.

Table 1. Molecular Characterization of the Four Block Copolymers

	$DP_{AETAI/NIPAM}$[a]	$M_{n,NMR}$[a] (g/mol)	$M_{n,SEC}$[b] (g/mol)	$Đ$[b]	LCST[c] (°C)
PAN11+	2/11	4000	2500	1.06	
PAN40+	2/40	7300	6500	1.09	65
PAN77+	2/77	11,500	12,100	1.10	67
PAN161+	2/161	21,000	22,600	1.14	58

[a]The DP of AETAI for each polymer was calculated by integrating the methylene group belonging to BTPA (peak a) and three methyl terminal groups of AETAI (peak j) after quaternization; DP of NIPAM for each polymer was calculated by integrating peak a, and combined protons from methylene group adjacent to the nitrogen [peak (i)] and methine group from NIPAM (peak l) after quaternization (Figures 1, S4−S6); $M_{n,NMR}$ for each polymer was calculated based on DPs of AETAI and NIPAM from NMR. [b]$M_{n,SEC}$ and $Đ$ were acquired by SEC in DMF using a refractive index detector before quaternization. [c]Measured by UV−vis spectroscopy at 500 nm transmittance.

2.2. Thermoresponsive Behavior of Cationic PFPE-Containing Block Copolymer Sorbents. The thermoresponsive properties of PAN polymers were explored to determine the LCST and aggregation behavior upon heating. In this work, the LCST was defined as the temperature at which the optical transmittance dropped by 90% of the initial value during the heating process. Though PNIPAM exhibits an LCST at ∼32 °C,[21,22] the presence of hydrophilic AETAI groups and the hydrophobic PFPE segment may alter the LCST of the block copolymers in aqueous solution. The thermoresponsive behavior of the four cationic PFPE-containing polymers, PAN11+, PAN40+, PAN77+, and

https://doi.org/10.1021/acs.macromol.4c01868
Macromolecules 2024, 57, 11166−11176

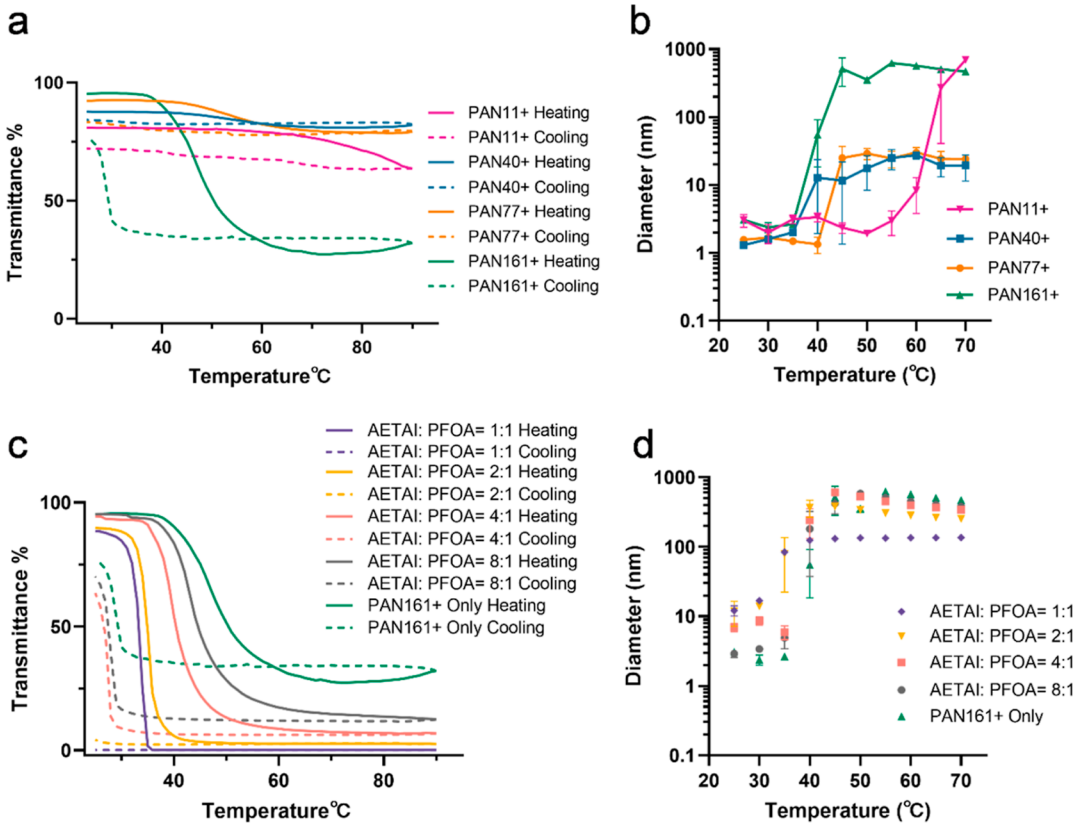

Figure 2. Thermoresponsive behavior of the four prepared pure block copolymers (a,b) and a typical polymer PAN161+ in the presence of different concentrations of PFOA (c,d) in Milli-Q water, measured by UV−vis (a,c) and DLS (b,d). Polymers, 10 mg/mL each; 1:1, 2:1, 4:1, and 8:1 represent mole ratios of AETAI of PAN161+ to PFOA. The results of DLS are the average of three measurements, and one standard error of the mean (SEM) is shown.

PAN161+ were examined at a fixed concentration of 10 mg/mL, using UV−vis spectroscopy across a temperature range of 25−90 °C. Figure 2a demonstrates that PAN161+ has the strongest phase transition upon heating based on the largest extent of decrease in transmittance within the temperature range. However, 0% transmittance was not reached for PAN161+ when the phase transition was fully complete, suggesting the role of quaternized ammonium groups that increase the solubility of PAN161+ in the aqueous solution.[32] The LCST of PAN161+ was subsequently calculated to be 58 °C (Table 1). For PAN11+, a phase transition was not observed until the temperature went beyond 60 °C and was the broad transition extended beyond 90 °C (Figure 2a), indicating a relatively high LCST. Both PAN40+ and PAN77+ showed weak phase transitions upon heating (Figure 2a), and the LCSTs of the polymer sorbents were calculated to be 65 and 67 °C, respectively (Table 1).

In LCST polymers, the balance between hydrophobic and hydrophilic segments largely determines the LCST. With DPs of NIPAM increasing from 11 to 161, the content of NIPAM increases from 31.1 to 86.8%, while the contents of AETAI and PFPE segments decrease from 14.3 to 2.7% and from 49.2 to 9.4%, respectively (Table S2). For each block copolymer, the molar amount (in mmol/g) of each of the above three functional groups normalized by the weight of the polymer was also calculated (Table S2). An increasing molar amount of NIPAM but decreasing molar amounts of AETAI and PFPE with increasing DPs of NIPAM aligns with the trend for the content of each functional group. The lowest LCST observed for PAN161+ among the four polymer sorbents is primarily due to the presence of the largest content of NIPAM but also the lowest content of the quaternized ammonium groups. This observation is supported by previous studies from Graillot et al.,[33,34] who observed decreasing LCST with decreasing amounts of hydrophilic moieties of phosphonic acid but increasing amounts of thermoresponsive units of *N*-*n*-propylacrylamide in the solution.

Dynamic light scattering (DLS) measurements provide detailed information about the size changes of PAN chains during the heating process. Temperature ranges were set from 25 to 70 °C. Figure 2b shows that before heating at 25 °C, the hydrodynamic diameter (D_h) for all polymers was ≤3.1 nm. Upon heating, increases in D_h were observed for the four polymer sorbents across various temperature ranges. No obvious increase in D_h of PAN11+ was observed below 55 °C. This was followed by a dramatic increase to ∼700 nm when the temperature increased to 70 °C, corresponding well with the phase transition of PAN11+ when the temperature was >60 °C from the UV−vis shown in Figure 2a. A significant increase in D_h from 3.1 to 513.8 nm was observed for PAN161+, while for PAN77+ and PAN40+, the increase in D_h was less significant, again, agreeing well with the observations of the weaker phase transitions of the two block copolymers from UV−vis (Figure 2a).

2.3. Thermoresponsive Behavior of PAN in the Presence of Different Concentrations of PFOA in Milli-Q. As mentioned above, the presence of quaternized ammonium groups from the prepared block copolymers can

https://doi.org/10.1021/acs.macromol.4c01868
Macromolecules 2024, 57, 11166−11176

significantly affect their solubility and LCSTs in aqueous solution. Here in this work, the influence of the concentration of PFAS on the thermal-responsive behavior of the block copolymer was examined using PFOA as a typical PFAS and PAN161+ as the sorbent. Upon mixing PFOA at different concentrations with PAN161+ at a fixed concentration of 10 mg/mL, the thermoresponsive behavior of the polymer sorbent was studied by performing both UV−vis and DLS experiments. In these solution mixtures, the mole ratios of AETAI to PFOA were 8:1, 4:1, 2:1, and 1:1. Before heating, i.e., at 25 °C, the results from Figure 2c show lower initial transmittance of the solution mixtures in the presence of higher concentrations of PFOA, 95.3%, 95.2%, 94.4%, 89.7%, and 88.4%, for no PFOA, and 8:1, 4:1, 2:1, and 1:1 AETAI to PFOA, respectively, indicating a more significant aggregation of PAN161+ after interacting with higher concentrations of PFOA. Upon heating, phase transitions occurred for all sample solutions, with both lower transmittance of the polymer solutions and LCSTs of PAN161+ being observed in the presence of increasing concentrations of PFOA (Table S3), mainly attributed to an increasing hydrophobicity of the polymer sorbent in the aqueous solution after interacting with increasing concentrations of PFOA.[31,35]

When the temperature cooled back to 25 °C, the results in Figure 2c demonstrate a partially reversable phase transition in the polymer solutions in the absence or in the presence of relatively low concentrations of PFOA, i.e., mole ratios of AETAI to PFOA of 8:1 and 4:1, and the phase transition was nearly permanent for the polymer solution in the presence of the two highest concentrations of PFOA, i.e., mole ratio of AETAI to PFOA of 2:1 and 1:1. The above observations of incomplete reversable phase transitions of the polymer solutions are attributed to hysteresis, mainly due to the formation of additional intrachain hydrogen bonding and hydrophobic interactions after phase transition.[36−38]

DLS size measurements conducted from 25 to 70 °C further substantiate the observations from UV−vis discussed above. Figure 2d shows that at 25 °C, aggregates with larger D_h formed in the presence of increasing concentrations of PFOA, i.e., 2.9, 6.9, 11.8, and 12.1 nm, corresponding to the mole ratio of AETAI to PFOA of 8:1, 4:1, 2:1, and 1:1, respectively. This aligns well with the decreasing initial transmittance observed in UV−vis (Figure 2c). Similar observations have been reported previously for either cationic PFPE-containing polymer in the presence of anionic PFOA, or anionic poly(acrylic acid)-based polymer with addition of cationic dodecyl trimethylammonium bromide,[31,39] demonstrating that high concentrations of counterions in solution lead to the formation of large aggregates due to electrostatic attraction. Upon heating to 70 °C, smaller values of D_h were observed for PAN161+ with increasing concentrations of PFOA after phase transitions, contrasting with the lower transmittance of the solution mixtures observed in UV−vis, as shown in Figure 2c. This might be due to larger amount of aggregates in solution that contributed to greater light intensity loss in turbidimetry.[40] In addition, the presence of PFOA reduced the temperature range over which significant increases in D_h of PAN161+ occurred, particularly evident when mole ratios of AETAI to PFOA were 2:1 and 1:1 (Figure 2d). To be more specific, a dramatic increase in D_h of PAN161+ was observed between 30 and 40 °C at AETAI to PFOA ratios of 2:1 and 1:1, whereas for solutions without PFOA or with AETAI to PFOA ratios of 4:1 and 8:1, similar increases were observed between 35 and 45 °C. The reduction in the temperature range in the presence of high concentrations of PFOA is roughly in line with the decreased LCSTs measured by UV−vis (Table S3). After phase transitions, the further increase in temperature for PAN161+ in the absence or in the presence of different concentrations of PFOA (except when AETAI to PFOA = 1:1) resulted in slight decreases in D_h of the polymer (Figure 2d). The finding is consistent with a previous work completed by Lemanowicz et al.,[41] who examined a copolymer containing NIPAM and methacrylic acid and reported a decreasing polymer size beyond the LCST due to the shrinkage of polymer aggregates from loose coils into compact, dehydrated globules. At a 1:1 mol ratio of AETAI to PFOA, PAN161+ showed little or no change in D_h upon heating from 40 to 70 °C, likely due to the formation of already hydrophobic and condensed globules during the phase transition process.

2.4. Investigation of the Influence of Variable Temperatures on the PFAS Sorption. The above results have demonstrated a crucial role of hydrophobicity/hydrophilicity balance within the polymer structure on its LCST, and such a balance could be affected by the presence of PFAS in the solution. However, determining a suitable temperature range for practical use of such thermoresponsive polymer sorbent for efficient removal of PFAS is critical. Previous studies have reported significant effects of high temperature on interactions of species in solution,[42−44] such as weakening electrostatic attraction between Bent and hydrolyzed poly(acrylamide/dimethyl diallyl ammonium chloride) and reducing intermolecular hydrogen bonding for a copolymer prepared using oligo(ethylene glycol)methyl ether methacrylate and 2,2,2-trifluoroethyl acrylate. Therefore, the temperature may play an important role in influencing the sorption of PFAS by our polymer sorbents.

Interactions between the thermoresponsive cationic fluorinated polymer sorbent and PFAS at the molecular level were investigated using variable temperature ^{19}F NMR spectroscopy analysis. PAN40+ was chosen as the typical sorbent due to (1) its high fluorine content that maximizes the fluorine signal in ^{19}F NMR spectra and (2) a weak phase transition upon heating that minimizes its precipitation above the LCST. PFOA and GenX were chosen as two typical PFAS for these experiments.

Figure 3 shows that at 25 °C, well-resolved peaks in the ^{19}F NMR spectra of both PFOA and GenX at 1.13 and 0.95 mg/mL were observed in the absence of PAN40+, indicating the complete dispersion of both PFAS molecules in solution. Upon addition of PAN40+ at 10 mg/mL (with a molar ratio AETAI/PFAS = 1:1), the ^{19}F resonances of PFAS shifted and broadened (Figure 3, Table S4). Taking PFOA as an example, the trifluoromethyl group [3F, $-CF_3$, peak (1)] at the chain end shifted from −80.76 to −82.99 ppm, accompanied by an increase in peak width at half height ($LW_{1/2}$) from 6.7 to 42.6 Hz. These changes in the chemical shift and peak width of PFOA after addition of PAN40+ are consistent with our previous studies[30,31] and indicate strong interactions between PFOA and the polymer sorbent via a combination of both fluorous and electrostatic interactions. Comparable observations were made for GenX, with notable line broadening of peak [2] from 8.0 to 115.2 Hz and peak [4] from 34.7 to 142.3 Hz in the presence of the polymer sorbent. The results from ^{19}F NMR confirm the presence of strong interactions between both the PFAS species and the PAN polymer.

The above solution mixture of either PFOA or GenX in the presence of PAN40+ was subsequently heated to 90 °C in

https://doi.org/10.1021/acs.macromol.4c01868
Macromolecules 2024, 57, 11166−11176

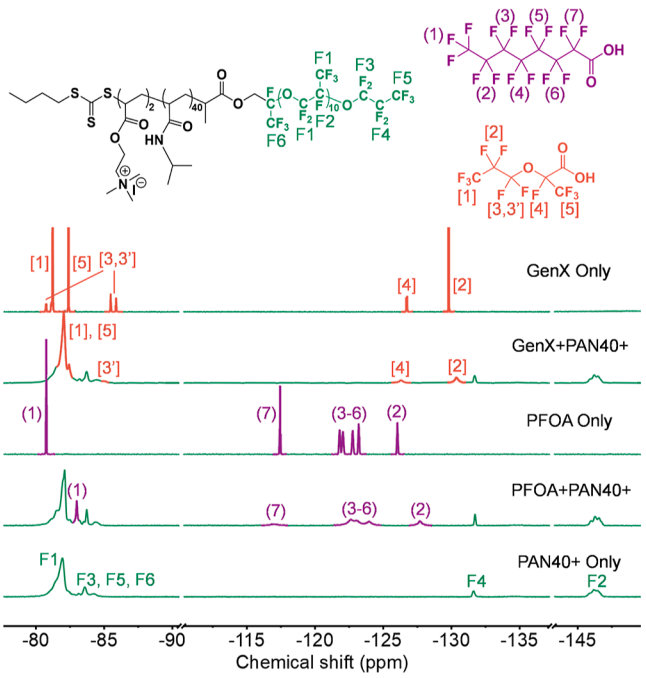

Figure 3. ^{19}F NMR spectra of PAN40+ only, PFOA only, GenX only, and PAN40+ in the presence of either PFOA or GenX in Milli-Q water at 25 °C (90% H_2O + 10% D_2O). Polymer, 10 mg/mL; PFOA, 1.13 mg/mL; and GenX, 0.95 mg/mL. Molar ratio of AETAI/PFAS = 1:1.

increments of 5 °C. The change in peak width of ^{19}F resonances of PFAS is an important indication of librational motion of the fluorinated segments in solution (Figure 4).[30] When PAN40+ was mixed with PFOA, the $LW_{1/2}$ of PFOA [peak (2)] increased from 123.5 to 485.7 Hz as the temperature rose from 25 to 40 °C (Figure 4c, purple). This suggests attenuated motion of the fluorinated segment of the PFAS, attributed to the phase transition of PAN40+ in the presence of PFOA in the solution. This finding was confirmed by UV−vis and DLS experiments using the same solution mixture (Figure S11a). At temperatures above 40 °C, a significant and continuous decrease in $LW_{1/2}$ of PFOA [peak (2)] was observed, indicating increasing librational motion of the PFAS, and can only be attributed to the continuous dissociation of initially bound PFOA from the polymer sorbent at higher temperatures. When GenX was examined in place of PFOA, similar observations were made by calculating $LW_{1/2}$ of peak [4] from the PFAS as the temperature increased from 25 to 90 °C (Figure 4c, red symbols). Initially, there was a general increase in $LW_{1/2}$ from 142.3 to 176.8 Hz up to 40 °C due to the phase transition (Figure S11b), followed by a continuous decrease to 42.8 Hz as the temperature reached 80 °C. A plateau in $LW_{1/2}$ was observed when the temperature exceeded 80 °C, indicating the completion of the dissociation process of GenX from PAN40+. Upon heating, GenX exhibited smaller $LW_{1/2}$ values at each temperature compared to PFOA. This difference is mainly due to the more hydrophilic nature of GenX, stemming from its shorter chain length and the presence of a C−O bond in its chemical structure.[45−47] The variable temperature ^{19}F NMR study clearly demonstrates that high temperatures at >40 °C may lead to desorption of PFAS compounds from sorbents.

2.5. Removal of 11 Different PFAS by a PAN Polymer Sorbent. PAN161+ was selected as the optimal polymer

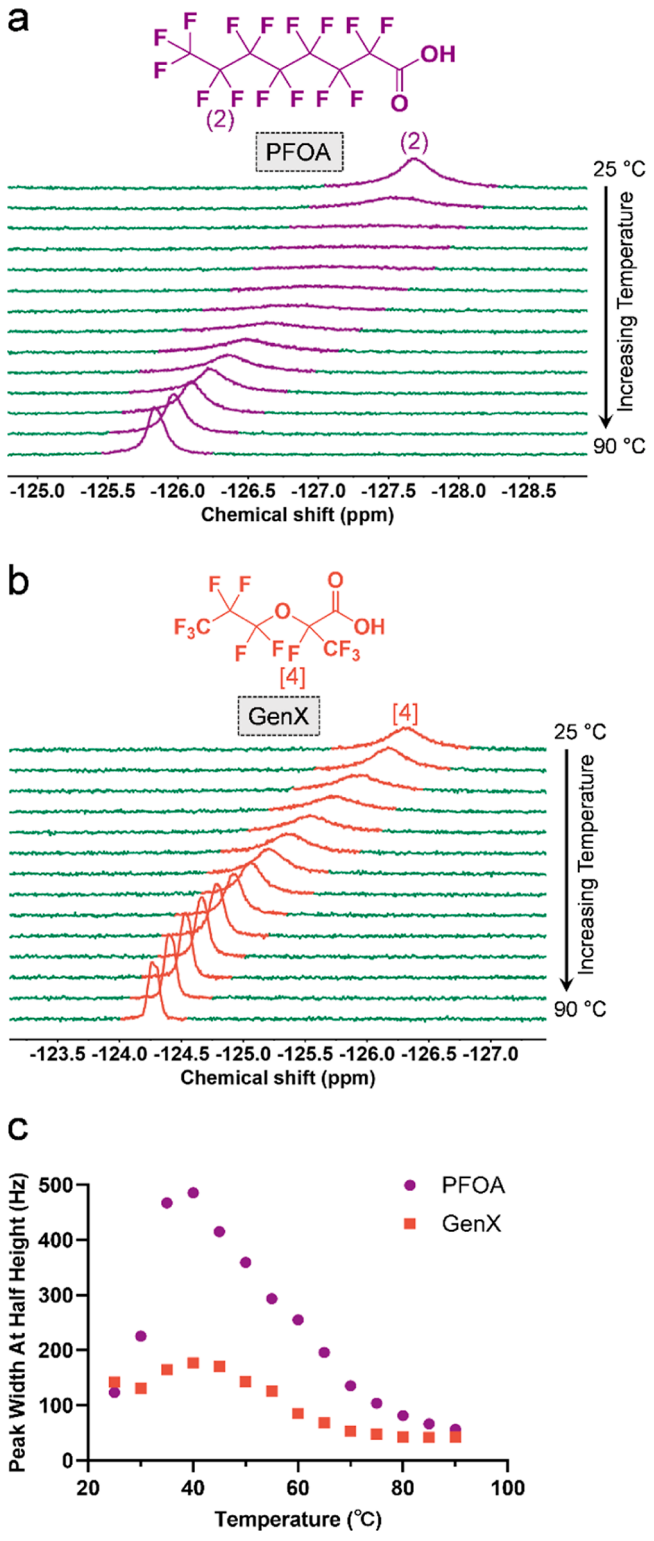

Figure 4. ^{19}F NMR analysis of PAN40+ in the presence of either PFOA or GenX with increased temperatures from 25 to 90 °C in Milli-Q water (90% H_2O + 10% D_2O). (a) Stacked ^{19}F NMR spectra of PFOA fluorine (2). (b) Stacked ^{19}F NMR spectra of GenX fluorine [4]. (c) Changes in peak width at half height of PFOA (peak (2)) and GenX (peak [4]) at different temperatures. Polymer, 10 mg/mL; PFOA, 1.13 mg/mL; and GenX, 0.95 mg/mL. The number of moles of PFOA or GenX equals that of AETAI of PAN40+. Changes in the chemical shift for PFOA, GenX, and PAN40+ were quantified and fitted well by a simple linear regression (Figure S12).[48,49]

https://doi.org/10.1021/acs.macromol.4c01868
Macromolecules 2024, 57, 11166−11176

sorbent for subsequent PFAS capture studies as it has a strong phase transition behavior and low LCST. In real water sources, complex components such as natural organic matter may largely compete for active sorption sites on the polymer sorbent,[50] potentially altering the thermoresponsive properties of the sorbent. Additionally, the presence of salt in the natural water could affect the LCST of the NIPAM-containing polymer.[51] To simulate these conditions, a PFAS stock solution containing 11 different kinds of PFAS at an initial concentration of 100 μg/L (ppb), each, was prepared in Milli-Q and supplemented with humic acid (HA) and sodium chloride (NaCl). After treatment using PAN161+ for 24 h, the thermoresponsive behavior of the sorbent was characterized using both UV−vis and DLS size measurements. Figure 5a (orange curves) demonstrates a low initial transmittance (18.4%) for the solution mixture before heating, indicating turbidity primarily due to the presence of HA and NaCl. This was confirmed by performing a control UV−vis experiment using the polymer solution with the same concentrations of HA and NaCl but in the absence of PFAS (Figure S13, orange). Upon heating to 45 °C, a further decrease in transmittance of the solution was observed due to the phase transition of the polymer sorbent (Figure 5a, orange), with the LCST estimated to be 40 °C.

The results from the DLS size measurements are consistent with those from UV−vis. At 25 °C, the D_h of PAN161+ was measured to be 27.6 nm (Figure 5a, blue), nine times larger than that of the pure polymer (3.1 nm) dissolved in Milli-Q (Figure 2d), indicating the formation of aggregates. A second DLS experiment using the polymer solution in the presence of the same concentrations of HA and NaCl but in the absence of PFAS showed a similar D_h of the polymer (~27.4 nm, Figure S13 blue), confirming that the increase in diameter of the polymer was due to the presence of HA and NaCl. Upon heating, a significant increase in the D_h of PAN161+ was observed between 30 and 40 °C (Figure 5a, blue), corresponding well with the phase transition behavior observed by UV−vis (Figure 5a, orange). At 40 °C, a maximum average D_h of 916.4 nm for the polymer sorbent was achieved, followed by a continuous decrease in D_h with a temperature up to 70 °C (Figure 5a, blue). The decrease in D_h for the polymer above LCST was attributed to a change in the conformation of the fluorinated aggregates, which is in line with the findings from the variable temperature DLS experiments shown in Figure 2d.

The removal of PAN161+ from water was evaluated by treating the polymer solution mixture at four different temperatures, i.e., 25, 40, 50, and 60 °C, followed by further filtration. As the poly(ether sulfone) (PES) membrane filter has been reported to withstand high temperatures,[52,53] a PES filter with an average pore size of 0.22 μm was used to remove large particles from the solution mixture at each temperature. Collected filtrates were analyzed by using ^{19}F NMR for quantification of the remaining PAN161+ after separation. Trifluoroethanol (TFE, 10%, v/v) in the presence of deuterium oxide (D_2O) filled in a coaxial inset was used as the internal standard. Figure 5b demonstrates that the filtrate collected at 25 °C had the highest content of PFPE [relative intensity to TFE (set as 100) = 21.93] among all of the four temperatures, indicating larger quantities of PAN161+ with smaller D_h passed through the PES filter. Upon heating, significantly decreased NMR intensity of PFPE in the filtrates collected at 40, 50, and 60 °C was observed, 0.22, 2.23, and 4.72 respectively, mainly ascribed to phase transitions and

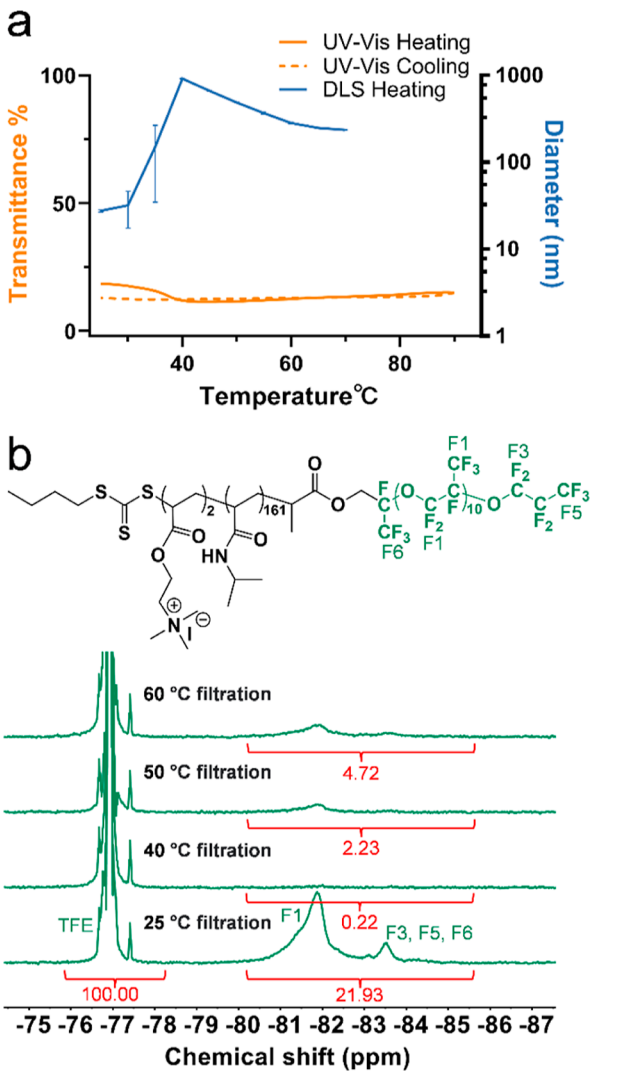

Figure 5. Thermoresponsive behavior of PAN161+ after sorption of 11 different PFAS in the presence of HA and NaCl. (a) Transmittance of the solution mixture and size changes of PAN161+ at varied temperatures; (b) ^{19}F NMR spectra of filtrates of PAN161+ prepared using filtration at different temperatures. Sorption duration: 24 h; PFAS initial concentration, 100 ppb each; and PAN161+, 10 mg/mL. Water constituents: Milli-Q in the presence of 20 ppm of HA and 200 ppm of NaCl, pH = 5.0. The results of DLS are the average of three measurements, and one SEM is shown. The samples were heated at the corresponding temperatures for 20 min before filtration. Coaxial inserts filled with D_2O/TFE (9/1, v/v) were used to lock the magnetic field. Treated temperatures: 25, 40, 50, and 60 °C.

increased D_hs of PAN161+ as demonstrated in Figure 5a. A much lower content of PFPE in the filtrate collected at 40 °C was observed compared with 50 and 60 °C, consistent with the DLS results in Figure 5a showing a continuous decreasing polymer size with the temperature further increasing to >40 °C, resulting in less polymer passing through the PES filters (Figure S14). The presence of residue PAN161+ at 40 °C was mainly ascribed to the nonuniform size of aggregates due to molecular-weight dispersity of the polymer, i.e., variation in DPs of AETAI and NIPAM.

The performance of PAN161+ in the removal of 11 PFAS was further examined by analyzing the above collected filtrates using liquid chromatography with tandem mass spectrometry

https://doi.org/10.1021/acs.macromol.4c01868
Macromolecules 2024, 57, 11166−11176

(LC−MS/MS). The 11 PFAS tested in this work can be classified as perfluoroalkyl carboxylic acids (PFCAs, $C_nF_{2n+1}COOH$), perfluoroalkyl sulfonic acids (PFSAs, $C_nF_{2n+1}SO_3H$), and GenX (Figure S15). At 25 °C, little-to-no removal of the 11 PFAS could be achieved after filtration of the solution mixture (Figure 6). This was mainly due to the

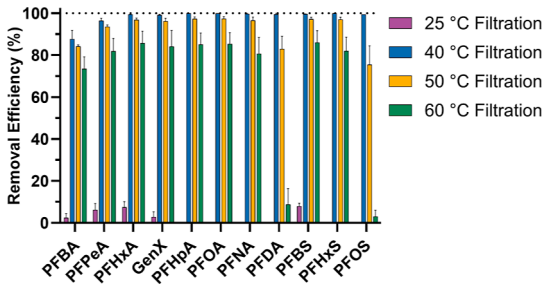

Figure 6. Removal efficiency of 11 different PFAS by PAN161+ after filtration at different temperatures. The samples were heated at the corresponding temperatures for 20 min before filtration. Sorption duration, 24 h; PFAS initial concentration, 100 ppb each; and PAN161+, 10 mg/mL. Water constituents: Milli-Q in the presence of 20 ppm of HA and 200 ppm of NaCl, pH = 5.0. Treated temperatures: 25, 40, 50, and 60 °C. The results are an average of three replicates, and one standard deviation is shown.

presence of water-soluble PAN161+ having small particle size that eluted together with the bound PFAS.[15,17,18] Upon heating the solution to above the phase transition at 40 °C, >99% of all tested PFAS was captured and removed after filtration using PES filters except two PFCAs, PFBA (number of fluorinated carbons, n = 3) and PFPeA (n = 4). The relatively low removal of 87.6% for PFBA and 96.4% for PFPeA was mainly due to the shorter chain lengths of these PFAS, largely increasing their hydrophilicity in the aqueous solution making them more difficult to be captured by the polymer sorbent. In addition, the removal of PFBS (99.5%) was non-negligibly higher than that of PFPeA with the two PFAS having the same number of fluorinated carbons (n = 4). This can be attributed to a combination of (1) the more hydrophobic nature of PFSA than PFCA that leads to stronger hydrophobic interactions between PFAS and the PFPE segments,[54] and (2) the stronger negative inductive effect of the sulfonate than the carboxylate due to resonance stabilization.[55]

As the temperature further increased to 50 and 60 °C, the decreased removal efficiency of PFAS is observed in Figure 6. There are several potential explanations for this observation. First, the decreased PAN161+ particle size and increased amount of PAN161+ passing through the membrane filter at high temperatures (e.g., 50 and 60 °C, Figure 5) could lead to increased PFAS levels in the filtrates. Second, as has been demonstrated in Figure 4, dissociation of two typical PFAS, PFOA and GenX, occurred when the temperature of the solution exceeded 40 °C. As a consequence, the dissociated PFAS could pass through the membrane filter and contribute to the lower PFAS removal efficiency at elevated temperatures.

The successful development of thermoresponsive polymer sorbent has several potential implications. First, it efficiently captures PFAS molecules from contaminated water sources through a combination of fluorous interactions and electrostatic attraction.[30,31,56] This not only increases the sorption selectivity for PFAS due to its fluorophilicity but also allows it to work effectively on multiple types of PFAS. Second, it enables easy separation of polymer sorbent from purified water solution using a simple heating and filtration process after sorption. Such a regeneration method eliminates the need for commonly used organic solvents and brine solutions, offering a more environmentally friendly alternative.

3. CONCLUSIONS

In summary, a series of thermoresponsive cationic perfluoropolyether (PFPE)-containing block copolymers with different contents of NIPAM were successfully prepared by RAFT polymerization. The PAN161+ polymer having the highest NIPAM content (86.8%) exhibits the most progressive phase transition and the lowest LCST (58 °C) among all prepared polymers. Lower LCSTs for PAN161+ were observed when interacting with PFOA due to the increased hydrophobicity of the polymer sorbent. Variable temperature ^{19}F NMR experiments indicate dissociation of PFAS from the polymer when the solution temperature exceeds 40 °C. In addition, capture experiments of 11 different PFAS (initial concentration 100 ppb each) in the presence of 20 ppm of HA and 200 ppm of NaCl by PAN161+ were performed. Upon complete sorption of PFAS, the sorbent exhibits an LCST of 40 °C and a particle size exceeding 900 nm above the LCST. The solution mixture was filtered at 40 °C, achieving a PFAS removal efficiency greater than 99% for the majority of the tested PFAS, and the PFAS removal efficiency is significantly higher compared to filtration at higher temperatures. Overall, this study offers key insights into designing efficient "smart" PFAS sorbents, utilizing their thermoresponsive properties for effective separation from aqueous solutions through a simple heating process.

■ ASSOCIATED CONTENT

Data Availability Statement

The data that support the findings of this study are available from the corresponding author upon reasonable request.

Supporting Information

The Supporting Information is available free of charge at https://pubs.acs.org/doi/10.1021/acs.macromol.4c01868.

Synthetic procedures and characterization methods; multiple reaction monitoring details for analytes and internal standards used for LC−MS/MS analysis; ^1H and ^{19}F NMR spectra with assignments; quantitative characterization of different functional groups of each prepared block copolymer; UV−vis results of PAN161+ in the absence or in the presence of different concentrations of PFOA after phase transitions in Milli-Q; $LW_{1/2}$ for PFOA and GenX peaks either in the absence or in the presence of PAN40+ in Milli-Q at 25 °C; ^{19}F NMR spectra, UV−vis, and DLS size measurements of PAN40+ in the presence of either PFOA or GenX at increasing temperatures; UV−vis and DLS size measurements of PAN161+ in the presence of HA and NaCl; ^{19}F NMR spectra of residue PAN161+ after filtration at 40 °C; and chemical structures of the 11 PFAS tested in this work (PDF)

■ AUTHOR INFORMATION

Corresponding Authors

Andrew K. Whittaker − *Australian Institute for Bioengineering and Nanotechnology, The University of*

https://doi.org/10.1021/acs.macromol.4c01868
Macromolecules 2024, 57, 11166−11176

Queensland, Brisbane, Queensland 4072, Australia; orcid.org/0000-0002-1948-8355; Email: a.whittaker@uq.edu.au

Cheng Zhang − *Australian Institute for Bioengineering and Nanotechnology, The University of Queensland, Brisbane, Queensland 4072, Australia; Centre for Advanced Imaging, The University of Queensland, Brisbane, Queensland 4072, Australia;* orcid.org/0000-0002-2722-7497; Email: c.zhang3@uq.edu.au

Authors

Xiao Tan − *Australian Institute for Bioengineering and Nanotechnology, The University of Queensland, Brisbane, Queensland 4072, Australia; Centre for Advanced Imaging, The University of Queensland, Brisbane, Queensland 4072, Australia;* orcid.org/0000-0002-9278-6068

Yiqing Wang − *Australian Institute for Bioengineering and Nanotechnology, The University of Queensland, Brisbane, Queensland 4072, Australia; Centre for Advanced Imaging, The University of Queensland, Brisbane, Queensland 4072, Australia*

Zhuojing Yang − *Australian Institute for Bioengineering and Nanotechnology, The University of Queensland, Brisbane, Queensland 4072, Australia; Centre for Advanced Imaging, The University of Queensland, Brisbane, Queensland 4072, Australia;* orcid.org/0000-0002-8925-8977

Yutong Zhu − *Australian Institute for Bioengineering and Nanotechnology, The University of Queensland, Brisbane, Queensland 4072, Australia; Centre for Advanced Imaging, The University of Queensland, Brisbane, Queensland 4072, Australia*

Chunrong Yu − *Australian Institute for Bioengineering and Nanotechnology, The University of Queensland, Brisbane, Queensland 4072, Australia; Centre for Advanced Imaging, The University of Queensland, Brisbane, Queensland 4072, Australia*

Kehan Liu − *Australian Institute for Bioengineering and Nanotechnology, The University of Queensland, Brisbane, Queensland 4072, Australia; Centre for Advanced Imaging, The University of Queensland, Brisbane, Queensland 4072, Australia*

Yutong He − *Australian Institute for Bioengineering and Nanotechnology, The University of Queensland, Brisbane, Queensland 4072, Australia; Centre for Advanced Imaging, The University of Queensland, Brisbane, Queensland 4072, Australia*

Complete contact information is available at: https://pubs.acs.org/10.1021/acs.macromol.4c01868

Notes

The authors declare no competing financial interest.

■ ACKNOWLEDGMENTS

The authors acknowledge the Australian Research Council (DP210101496 and LP220100036) and The University of Queensland Knowledge Exchange & Translation Grant for funding of this research. C.Z. acknowledges the Australian Research Council for his Discovery Early Career Researcher Award fellowship (DE230101105). The Australian National Fabrication Facility, Queensland Node, is acknowledged for access to some items of equipment. The Chemours Company is also acknowledged for providing perfluoropolyether.

■ REFERENCES

(1) Panieri, E.; Baralic, K.; Djukic-Cosic, D.; Buha Djordjevic, A.; Saso, L. PFAS Molecules: A Major Concern for the Human Health and the Environment. *Toxics* **2022**, *10*, 44.

(2) Ehsan, M. N.; Riza, M.; Pervez, M. N.; Khyum, M. M. O.; Liang, Y. N.; Naddeo, V. Environmental and health impacts of PFAS: Sources, distribution and sustainable management in North Carolina (USA). *Sci. Total Environ.* **2023**, *878*, 163123.

(3) Cousins, I. T.; DeWitt, J. C.; Gluge, J.; Goldenman, G.; Herzke, D.; Lohmann, R.; Ng, C. A.; Scheringer, M.; Wang, Z. Y. The high persistence of PFAS is sufficient for their management as a chemical class. *Environ. Sci.: Processes Impacts* **2020**, *22*, 2307−2312.

(4) Kelly, B. C.; Ikonomou, M. G.; Blair, J. D.; Surridge, B.; Hoover, D.; Grace, R.; Gobas, F. A. P. C. Perfluoroalkyl Contaminants in an Arctic Marine Food Web: Trophic Magnification and Wildlife Exposure. *Environ. Sci. Technol.* **2009**, *43*, 4037−4043.

(5) Balan, S. A.; Mathrani, V. C.; Guo, D. F. M.; Algazi, A. M. Regulating PFAS as a Chemical Class under the California Safer Consumer Products Program. *Environ. Health Perspect.* **2021**, *129*, 025001.

(6) Lee, J. E.; Choi, K. Perfluoroalkyl substances exposure and thyroid hormones in humans: epidemiological observations and implications. *Ann. Pediatr. Endocrinol. Metab.* **2017**, *22*, 6−14.

(7) Granum, B.; Haug, L. S.; Namork, E.; Stolevik, S. B.; Thomsen, C.; Aaberge, I. S.; van Loveren, H.; Lovik, M.; Nygaard, U. C. Pre-natal exposure to perfluoroalkyl substances may be associated with altered vaccine antibody levels and immune-related health outcomes in early childhood. *J. Immunot.* **2013**, *10*, 373−379.

(8) Huang, Q.; Zhang, J.; Martin, F. L.; Peng, S.; Tian, M.; Mu, X.; Shen, H. Perfluorooctanoic acid induces apoptosis through the p53-dependent mitochondrial pathway in human hepatic cells: A proteomic study. *Toxicol. Lett.* **2013**, *223*, 211−220.

(9) Kataria, A.; Trachtman, H.; Malaga-Dieguez, L.; Trasande, L. Association between perfluoroalkyl acids and kidney function in a cross-sectional study of adolescents. *Environ. Health Global* **2015**, *14*, 89−13.

(10) Yuan, Y.; Ding, X.; Cheng, Y.; Kang, H.; Luo, T.; Zhang, X.; Kuang, H.; Chen, Y.; Zeng, X.; Zhang, D. PFOA evokes extracellular Ca^{2+} influx and compromises progesterone-induced response in human sperm. *Chemosphere* **2020**, *241*, 125074.

(11) Koda, Y.; Terashima, T.; Nomura, A.; Ouchi, M.; Sawamoto, M. Fluorinated microgel-core star polymers as fluorous compartments for molecular recognition. *Macromolecules* **2011**, *44*, 4574−4578.

(12) Koda, Y.; Terashima, T.; Sawamoto, M. Fluorous microgel star polymers: selective recognition and separation of polyfluorinated surfactants and compounds in water. *J. Am. Chem. Soc.* **2014**, *136*, 15742−15748.

(13) Koda, Y.; Terashima, T.; Takenaka, M.; Sawamoto, M. Star Polymer Gels with Fluorinated Microgels via Star-Star Coupling and Cross-Linking for Water Purification. *ACS Macro Lett.* **2015**, *4*, 377−380.

(14) Quan, Q.; Wen, H.; Han, S.; Wang, Z.; Shao, Z.; Chen, M. Fluorous-Core Nanoparticle-Embedded Hydrogel Synthesized via Tandem Photo-Controlled Radical Polymerization: Facilitating the Separation of Perfluorinated Alkyl Substances from Water. *ACS Appl. Mater. Interfaces* **2020**, *12*, 24319−24327.

(15) Kumarasamy, E.; Manning, I. M.; Collins, L. B.; Coronell, O.; Leibfarth, F. A. Ionic Fluorogels for Remediation of Per- and Polyfluorinated Alkyl Substances from Water. *ACS Cent. Sci.* **2020**, *6*, 487−492.

(16) Zhang, C.; Yan, K.; Fu, C.; Peng, H.; Hawker, C. J.; Whittaker, A. K. Biological Utility of Fluorinated Compounds: from Materials Design to Molecular Imaging, Therapeutics and Environmental Remediation. *Chem. Rev.* **2022**, *122*, 167−208.

(17) He, Y. T.; Cheng, X. R.; Gunjal, S. J.; Zhang, C. Advancing PFAS Sorbent Design: Mechanisms, Challenges, and Perspectives. *ACS Mater. Au* **2024**, *4*, 108−114.

(18) Tan, X.; Dewapriya, P.; Prasad, P.; Chang, Y.; Huang, X.; Wang, Y.; Gong, X.; Hopkins, T. E.; Fu, C.; Thomas, K. V.; Peng, H.;

Whittaker, A. K.; Zhang, C. Efficient Removal of Perfluorinated Chemicals from Contaminated Water Sources Using Magnetic Fluorinated Polymer Sorbents. *Angew. Chem., Int. Ed.* **2022**, *61*, No. e202213071.
(19) Lanzalaco, S.; Armelin, E. Poly(N-isopropylacrylamide) and Copolymers: A Review on Recent Progresses in Biomedical Applications. *Gels* **2017**, *3*, 36.
(20) Doberenz, F.; Zeng, K.; Willems, C.; Zhang, K.; Groth, T. Thermoresponsive polymers and their biomedical application in tissue engineering—a review. *J. Mater. Chem. B* **2020**, *8*, 607−628.
(21) Winnik, F. M. Fluorescence Studies of Aqueous Solutions of Poly(N-isopropylacrylamide) below and above Their Lcst. *Macromolecules* **1990**, *23*, 233−242.
(22) Ono, Y.; Shikata, T. Hydration and Dynamic Behavior of Poly(N-isopropylacrylamide)s in Aqueous Solution: A Sharp Phase Transition at the Lower Critical Solution Temperature. *J. Am. Chem. Soc.* **2006**, *128*, 10030−10031.
(23) Sanz, B.; von Bilderling, C.; Tuninetti, J. S.; Pietrasanta, L.; Mijangos, C.; Longo, G. S.; Azzaroni, O.; Giussi, J. M. Thermally-induced softening of PNIPAm-based nanopillar arrays. *Soft Matter* **2017**, *13*, 2453−2464.
(24) Liu, R. X.; Fraylich, M.; Saunders, B. R. Thermoresponsive copolymers: from fundamental studies to applications. *Colloid Polym. Sci.* **2009**, *287*, 627−643.
(25) Lee, M. S.; Kim, J. C. Effects of Surfactants on Phase Transition of Poly(N-isopropylacrylamide) and Poly(N-isopropylacrylamide-co-dimethylaminoethylmethacrylate). *J. Dispersion Sci. Technol.* **2012**, *33*, 272−277.
(26) Zhang, J.; Pelton, R. The Surface Tension of Aqueous Poly(N-isopropylacrylamide-co-acrylamide). *J. Polym. Sci., Part A: Polym. Chem.* **1999**, *37*, 2137−2143.
(27) Maeda, T.; Yamamoto, K.; Aoyagi, T. Importance of bound water in hydration-dehydration behavior of hydroxylated poly (N-isopropylacrylamide). *J. Colloid Interface Sci.* **2006**, *302*, 467−474.
(28) Cao, Z. Q.; Liu, W. G.; Gao, P.; Yao, K. D.; Li, H. X.; Wang, G. C. Toward an understanding of thermoresponsive transition behavior of hydrophobically modified N-isopropylacrylamide copolymer solution. *Polymer* **2005**, *46*, 5268−5277.
(29) Garcia-Penas, A.; Biswas, C. S.; Liang, W. J.; Wang, Y.; Yang, P. P.; Stadler, F. J. Effect of Hydrophobic Interactions on Lower Critical Solution Temperature for Poly(N-isopropylacrylamide-co-dopamine Methacrylamide) Copolymers. *Polymers* **2019**, *11*, 991.
(30) Tan, X.; Zhong, J.; Fu, C.; Dang, H.; Han, Y.; Král, P.; Guo, J.; Yuan, Z.; Peng, H.; Zhang, C.; Whittaker, A. K. Amphiphilic Perfluoropolyether Copolymers for the Effective Removal of Polyfluoroalkyl Substances from Aqueous Environments. *Macromolecules* **2021**, *54*, 3447−3457.
(31) Tan, X.; Sawczyk, M.; Chang, Y.; Wang, Y.; Usman, A.; Fu, C.; Král, P.; Peng, H.; Zhang, C.; Whittaker, A. K. Revealing the Molecular-Level Interactions between Cationic Fluorinated Polymer Sorbents and the Major PFAS Pollutant PFOA. *Macromolecules* **2022**, *55*, 1077−1087.
(32) Nonaka, T.; Hua, L.; Ogata, T.; Kurihara, S. Synthesis of water-soluble thermosensitive polymers having phosphonium groups from methacryloyloxyethyl trialkyl phosphonium chlorides-N-isopropylacrylamide copolymers and their functions. *J. Appl. Polym. Sci.* **2003**, *87*, 386−393.
(33) Graillot, A.; Bouyer, D.; Monge, S.; Robin, J. J.; Faur, C. Removal of nickel ions from aqueous solution by low energy-consuming sorption process involving thermosensitive copolymers with phosphonic acid groups. *J. Hazard. Mater.* **2013**, *244*−*245*, 507−515.
(34) Graillot, A.; Monge, S.; Faur, C.; Bouyer, D.; Duquesnoy, C.; Robin, J. J. How to easily adapt cloud points of statistical thermosensitive polyacrylamide-based copolymers knowing reactivity ratios. *RSC Adv.* **2014**, *4*, 19345−19355.
(35) Wang, Y. C.; Li, Y.; Yang, X. Z.; Yuan, Y. Y.; Yan, L. F.; Wang, J. Tunable Thermosensitivity of Biodegradable Polymer Micelles of Poly (ε-caprolactone) and Polyphosphoester Block Copolymers. *Macromolecules* **2009**, *42*, 3026−3032.
(36) Wu, C.; Wang, X. H. Globule-to-Coil Transition of a Single Homopolymer Chain in Solution. *Phys. Rev. Lett.* **1998**, *80*, 4092−4094.
(37) Cheng, H.; Shen, L.; Wu, C. LLS and FTIR Studies on the Hysteresis in Association and Dissociation of Poly(N-isopropylacrylamide) Chains in Water. *Macromolecules* **2006**, *39*, 2325−2329.
(38) Mori, T.; Beppu, S.; Berber, M. R.; Mori, H.; Makimura, T.; Tsukamoto, A.; Minagawa, K.; Hirano, T.; Tanaka, M.; Niidome, T.; Katayama, Y.; Hirano, T.; Maeda, Y. Design of Temperature-Responsive Polymers with Enhanced Hysteresis: α,α-Disubstituted Vinyl Polymers. *Langmuir* **2010**, *26*, 9224−9232.
(39) Wang, C.; Tam, K. C. New Insights on the Interaction Mechanism within Oppositely Charged Polymer/Surfactant Systems. *Langmuir* **2002**, *18*, 6484−6490.
(40) Kleizen, H. H.; Deputter, A. B.; Vanderbeek, M.; Huynink, S. J. Particle Concentration, Size and Turbidity. *Filtr. Sep.* **1995**, *32*, 897−901.
(41) Lemanowicz, M.; Gierczycki, A.; Kuznik, W.; Sancewicz, R.; Imiela, P. Determination of Lower Critical Solution Temperature of thermosensitive flocculants. *Miner. Eng.* **2014**, *69*, 170−176.
(42) You, Z. J.; Bedrikovetsky, P.; Badalyan, A.; Hand, M. Particle mobilization in porous media: Temperature effects on competing electrostatic and drag forces. *Geophys. Res. Lett.* **2015**, *42*, 2852−2860.
(43) Lin, L.; Luo, P. Y. Effect of polyampholyte-bentonite interactions on the properties of saltwater mud. *Appl. Clay Sci.* **2018**, *163*, 10−19.
(44) Zhang, C.; Peng, H.; Whittaker, A. K. NMR Investigation of Effect of Dissolved Salts on the Thermoresponsive Behavior of Oligo(ethylene glycol)-Methacrylate-Based Polymers. *J. Polym. Sci., Part A: Polym. Chem.* **2014**, *52*, 2375−2385.
(45) Wang, W.; Maimaiti, A.; Shi, H.; Wu, R.; Wang, R.; Li, Z.; Qi, D.; Yu, G.; Deng, S. Adsorption behavior and mechanism of emerging perfluoro-2-propoxypropanoic acid (GenX) on activated carbons and resins. *Chem. Eng. J.* **2019**, *364*, 132−138.
(46) Wen, J.; Li, H.; Ottosen, L. D. M.; Lundqvist, J.; Vergeynst, L. Comparison of the photocatalytic degradability of PFOA, PFOS and GenX using Fe-zeolite in water. *Chemosphere* **2023**, *344*, 140344.
(47) Rice, P. A.; Cooper, J.; Koh-Fallet, S. E.; Kabadi, S. V. Comparative analysis of the physicochemical, toxicokinetic, and toxicological properties of ether-PFAS. *Toxicol. Appl. Pharmacol.* **2021**, *422*, 115531.
(48) Mysegaes, F.; Spiteller, P.; Bernarding, J.; Plaumann, M. ^{19}F VT NMR: Novel $Tm^{3+}$and Ce^{3+} Complexes Provide New Insight into Temperature Measurement Using Molecular Sensors. *ChemPhysChem* **2023**, *24*, No. e202300057.
(49) Prinz, C.; Delgado, P. R.; Eigentler, T. W.; Starke, L.; Niendorf, T.; Waiczies, S. Toward ^{19}F magnetic resonance thermometry: spin−lattice and spin−spin-relaxation times and temperature dependence of fluorinated drugs at 9.4 T. *Magn. Reson. Mater. Phys., Biol. Med.* **2019**, *32*, 51−61.
(50) Adou, A. F.; Muhandiki, V. S.; Shimizu, Y.; Matsui, S. A new economical method to remove humic substances in water: adsorption onto a recycled polymeric material with surfactant addition. *Water Sci. Technol.* **2001**, *43*, 1−7.
(51) Du, H. B.; Wickramasinghe, R.; Qian, X. H. Effects of Salt on the Lower Critical Solution Temperature of Poly (N-Isopropylacrylamide). *J. Phys. Chem. B* **2010**, *114*, 16594−16604.
(52) Rahimpour, A.; Madaeni, S. S.; Amirinejad, M.; Mansourpanah, Y.; Zereshki, S. The effect of heat treatment of PES and PVDF ultrafiltration membranes on morphology and performance for milk filtration. *J. Membr. Sci.* **2009**, *330*, 189−204.
(53) Yousef, S.; Sereika, J.; Tonkonogovas, A.; Hashem, T.; Mohamed, A. CO_2/CH_4, CO_2/N_2 and CO_2/H_2 selectivity performance of PES membranes under high pressure and temperature for biogas upgrading systems. *Environ. Technol. Innovat.* **2021**, *21*, 101339.

https://doi.org/10.1021/acs.macromol.4c01868
Macromolecules 2024, 57, 11166−11176

(54) Li, R.; Alomari, S.; Islamoglu, T.; Farha, O. K.; Fernando, S.; Thagard, S. M.; Holsen, T. M.; Wriedt, M. Systematic Study on the Removal of Per- and Polyfluoroalkyl Substances from Contaminated Groundwater Using Metal-Organic Frameworks. *Environ. Sci. Technol.* **2021**, *55*, 15162−15171.
(55) Park, M.; Daniels, K. D.; Wu, S.; Ziska, A. D.; Snyder, S. A. Magnetic ion-exchange (MIEX) resin for perfluorinated alkylsubstance (PFAS) removal in groundwater: Roles of atomic charges for adsorption. *Water Res.* **2020**, *181*, 115897.
(56) Yang, Z.; Zhu, Y.; Tan, X.; Gunjal, S. J. J.; Dewapriya, P.; Wang, Y.; Xin, R.; Fu, C.; Liu, K.; Macintosh, K.; et al. Fluoropolymer sorbent for efficient and selective capturing of per- and polyfluorinated compounds. *Nat. Commun.* **2024**, *15* (1), 8269.

https://doi.org/10.1021/acs.macromol.4c01868
Macromolecules 2024, 57, 11166−11176